Particulate phases are key in controlling dissolved iron concentrations in the (sub)-tropical North Atlantic

Angela Milne[1*], Christian Schlosser[2,3], Bronwyn D. Wake[2], Eric P. Achterberg[2,3], Rosie Chance[4], Alex R. Baker[4], Alex Forryan[2] and Maeve C. Lohan[1]

[1]School of Geography, Earth and Environmental Sciences, Plymouth University, Plymouth, PL4 8AA, UK

[2]Ocean and Earth Sciences, National Oceanography Centre, University of Southampton, Southampton, SO14 3ZH, UK

[3]GEOMAR Helmholtz Centre for Ocean Research, 24148 Kiel, Germany

[4]Centre for Ocean and Atmospheric Sciences, School of Environmental Sciences, University of East Anglia, Norwich, Norfolk, NR4 7TJ, UK

Present addresses: Department of Chemistry, University of York, Heslington, York, YO10 5DD, UK (R.C). Ocean and Earth Sciences, National Oceanography Centre, University of Southampton, Southampton, SO14 3ZH, UK (M.C.L).

*Corresponding author: Angela Milne (angela.milne@plymouth.ac.uk)

Key points:

- Labile-particulate iron has a key role in iron cycling and can increase the overall 'available' iron pool by up to 55% in the OMZ.
- A strong relationship between particles and dissolved iron indicates that L-pFe 'buffers' the elevated dFe concentrations observed.
- Lateral shelf transport of available iron (L-pFe + dFe) supplied a similar magnitude of iron as atmospheric sources.

Abstract

The supply and bioavailability of iron (Fe) controls primary productivity and N_2-fixation in large parts of the global ocean. An important, yet poorly quantified, source to the ocean is particulate Fe (pFe). Here we present the first combined dataset of particulate, labile-particulate (L-pFe) and dissolved Fe (dFe) from the (sub)-tropical North Atlantic. We show a strong relationship between L-pFe and dFe, indicating a dynamic equilibrium between these two phases whereby particles 'buffer' dFe and maintain the elevated concentrations observed. Moreover, L-pFe can increase the overall 'available' (L-pFe + dFe) Fe pool by up to 55%. The lateral shelf flux of this available Fe was similar in magnitude to observed soluble aerosol-Fe deposition, a comparison that has not been previously considered. These findings demonstrate that L-pFe is integral to Fe cycling and hence plays a role in regulating carbon cycling, warranting its' inclusion in Fe budgets and biogeochemical models.

1. Introduction

Iron (Fe) is an essential micronutrient for the growth of phytoplankton and hence plays a crucial role in ocean ecosystems [*Boyd and Ellwood*, 2010]. It is required for key metabolic functions such as photosynthesis, and nitrogen (N_2) fixation [*Morel et al.*, 2003; *Sunda*, 2001; *Whitfield*, 2001]. The sensitivity of ecosystems to Fe supply is related to its short residence time, which is in the order of days to months in surface waters and tens to a few hundred years in deep waters [*Bergquist et al.*, 2007; *Bruland et al.*, 1994]. The dissolved phase (dFe) is considered the most biologically available fraction [*Wells et al.*, 1995], however, the main flux of Fe to the ocean is in the particulate form (i.e. dust deposition, river transport, sediment re-suspension, off-shelf transport, ice-rafted debris). The oceanic Fe inventory in shelf systems is dominated by the particulate phase (pFe) [*Hong and Kester*, 1986; *Lippiatt et al.*, 2010], yet the cycling of this fraction in shelf or open ocean environments is not well constrained. In oxygenated seawater, the predominant Fe species, Fe(III), is highly insoluble and precipitates to form particulate phases, [*Sunda*, 2001; *Wu and Luther*, 1994]. This process is mitigated by the presence of natural organic ligands which complex ~ 99% of dFe and hence regulate dFe concentrations [*Gledhill and van den Berg*, 1994; *Rue and Bruland*, 1995]. Scavenging and precipitation of Fe to particulate phases result in losses of dFe. However, a surface-bound labile-pFe (L-pFe) fraction is considered to be involved in adsorption/desorption processes [*Homoky et al.*, 2012] with Fe becoming available to phytoplankton following dissolution and solubilization [*Hurst et al.*, 2010; *Lippiatt et al.*, 2010]. This fraction can include acid-labile hydroxides and biogenic particles as well as surface bound forms of Fe. Scavenging and dissolution interactions between L-pFe and dFe, plus remineralization from biogenic particles, may govern the distribution of dFe in the ocean.

In the North Atlantic, mineral dust forms the principal source of soluble and bioavailable Fe to surface waters [*Jickells et al.*, 2005; *Schlosser et al.*, 2014]. Additionally, continental margins and shelf sediments are significant sources of Fe to the ocean [*Elrod et al.*, 2004; *Lam and Bishop*, 2008] and can dominate the Fe budget on a global scale [*Tagliabue et al.*, 2014]. Inputs of particulate material from margins and Fe from enriched pore waters, not only sustains productivity in shallow coastal waters [*Hurst et al.*, 2010], but also supplies Fe to the ocean interior, either through lateral advection [*Lam et al.*, 2006] or mesoscale eddy transport [*Boyd et al.*, 2012; *Lippiatt et al.*, 2011].

We quantified the distributions of L-pFe, pFe and dFe in the (sub)-tropical Northeast Atlantic and explored the role of particles on the distribution of dFe. Atmospheric deposition [*Ohnemus and Lam*, 2015; *Powell et al.*, 2015], lateral advection of Fe from the eastern continental margin [*Conway and John*, 2014; *Rijkenberg et al.*, 2012], and inputs from benthic nepheloid layers [*Lam et al.*, 2015] all supply particulate Fe to this region. Here we present the first combined dataset of these three Fe fractions.

2. Materials and Methods

2.1 Sample collection and pre-treatment

Samples were collected during the GEOTRACES GA06 section in the (sub)-tropical Northeast Atlantic (Fig. 1a) from 7th February-19th March, 2011. Particulate samples were collected onto acid clean 25 mm Supor® polyethersulfone membrane disc filters (Pall, 0.45 µm) and stored frozen (-20ºC) until shore-based analysis. Seawater samples were filtered using 0.8/0.2 µm cartridge filters (AcroPak500/1000^{TM}), acidified to 0.013 M with high purity HCl (Romil, UpA) and allowed to equilibrate for at least 24 hours prior to on-board analysis. In a land-based laboratory, the labile-particle fraction of Fe and aluminum (Al) was determined using the protocol of Berger et al. [2008]. For determination of total pFe and

pAl, a sequential acid digestion modified from Ohnemus et al. [2014] was used. Full details in Supplementary Methods 1.

2.2 Sample Analyses

All particle samples were analyzed using inductively coupled plasma-mass spectrometry (Thermo Fisher XSeries-2). Potential interferences (e.g. $^{40}Ar^{16}O$ on ^{56}Fe) were minimized through the use of a collision/reaction cell utilizing 7% H in He. Evaluation of the leach and digestion efficiencies was made using four CRMs with the results showing good agreement (Table S1). Dissolved Fe was determined using flow-injection analysis with chemiluminescence detection [*Klunder et al.*, 2011; *Obata et al.*, 1993].

2.3 Atmospheric sampling and analysis

Clean aerosol samples were collected using a high volume (~1 m^3 min^{-1}) collector equipped with a 3-stage Sierra-type cascade impactor head. Sample filters were stored frozen (-20^{o}C) until shore-based analysis. Soluble aerosol Fe and Al were determined as detailed in Baker et al. [2007]. Total Fe and Al were determined by instrumental neutron activation analysis following protocols detailed in Baker et al. [2013]. Concentrations were converted to dry deposition fluxes by multiplying by the deposition velocity (V_d). Soluble aerosol concentrations were multiplied by a wind-speed dependent value of V_d (calculated using the method of *Ganzevald et al*. [1998]) assuming an aerodynamic diameter of 5 μm for the coarse mode (sampling cut-off of >1 μm) and 0.6 μm for the fine mode (cut-off of <1 μm). Total aerosol Fe and Al concentrations were only determined for bulk aerosol and so a single value of V_d (0.3 cm s^{-1}) was used. Further details in Supplementary Methods 2.

126 **2.4 Horizontal fluxes and vertical eddy diffusivity**

127 The offshore horizontal flux of Fe was estimated from the averaged decreasing
128 concentrations, moving away from the continental shelf, taken from depths below the mixed
129 layer to 500 m. The same potential density gradients were followed from the coast to the
130 open ocean and encompassed the highest concentrations of dFe in the OMZ. To calculate
131 estimates of the horizontal flux, a simplified one dimensional advective/diffusion model,
132 $\frac{\partial(Fe)}{\partial t} = -u\left(\frac{\partial(Fe)}{\partial x}\right) + K_h\left(\frac{\partial x^2(Fe)}{\partial x^2}\right) + J_h$, was applied [*de Jong et al.*, 2012; *Glover et al.*,
133 2011]. The vertical flux of Fe (J_Z) in the upper water column was calculated as detailed in
134 Jickells [1999] following the equation $J_Z = w\lceil Fe\rceil_{BML} + K_Z\frac{\partial Fe}{\partial z}$. Full details in
135 Supplementary Methods 3.
136
137 **3. Results and discussion**
138 **3.1 Distribution and sources of Fe**
139 Maximum concentrations of pFe (up to 140 nM), and pAl (up to 800 nM) as an
140 indicator of mineral particle input [*Duce et al.*, 1991], were observed close to the continental
141 margin whilst elevated values occurred across the full extent of the shelf slope (pFe: 10-50
142 nM, pAl: 50-200 nM; Fig. 1b-c). A key feature of our study area is the oxygen minimum
143 zone (Fig. S1) which extends from ~100-1000 m and was associated with enhanced dFe
144 concentrations >1 nM (Fig. 1d). Neither the pFe nor the pAl distributions were influenced by
145 low oxygen concentrations (41.2 to ~100 µmol kg^{-1}), indicating no influence on particle
146 formation, dissolution and cycling. Instead particle distributions were controlled by input
147 (continental margin/atmosphere) and removal (remineralization/sedimentation) processes as
148 reported in previous studies of this region [*Ohnemus and Lam*, 2015; *Revels et al.*, 2015].
149 The observed pFe/pAl mole ratios in waters adjacent to the shelf (<100 km from the African
150 coast) ranged between 0.17–0.21 (Fig. 1e), values which are similar to upper crustal mole

ratios (0.19–0.23 [*McLennan*, 2001; *Rudnick and Gao*, 2003; *Wedepohl*, 1995]). Interestingly, raised pFe (5-8 nM) and pAl (20–33 nM) concentrations, typical from intermediate nepheloid layers (INLs), were observed ~200 km from the coast at station 6. The pFe/pAl ratio in these two layers was 0.23 and 0.25 (Fig. 1e), whilst the average water column ratio at station 6 was 0.27 ± 0.02 (*n*=21). The low ratios in the INLs suggest that the higher pFe and pAl signals also originated from the shelf. The overall concentrations of pFe and pAl in the western water column were significantly lower (Mann Whitney Rank Sum Test, $P<0.001$) than in the eastern stations (2-6), and their distribution through the water column was relatively uniform (pFe: 1-3 nM; pAl: 5-10 nM). Here, the pFe/pAl ratios were higher than the overall average values observed east of station 6, averaging 0.30 ± 0.04 (*n*=80) compared to 0.25 ± 0.06 (*n*=59). Neither set of values are statistically different to the mean Fe/Al mole ratio of 0.27 ± 0.04 (total dry deposition, *n*=8) for our aerosol samples, which is also within the range previously reported for Saharan aerosols (0.26-0.37 [*Baker et al.*, 2013; *Formenti et al.*, 2003; *Shelley et al.*, 2015]). Large quantities of mineral dust are delivered to the North Atlantic through wet and dry deposition [*Baker et al.*, 2013; *Jickells et al.*, 2005; *Powell et al.*, 2015]. While no wet deposition was observed, dry deposition provided large and variable total (11645 ± 5985 nmol m^{-2} d^{-1}) and soluble (112 ± 72 nmol m^{-2} d^{-1}) aerosol Fe fluxes (*n*=8) which are typical for this region [*Rijkenberg et al.*, 2012; *Ussher et al.*, 2013]. This indicates that dust was a significant source of particulate material, in agreement with other studies of this region [*Conway and John*, 2014; *Revels et al.*, 2015].

3.2 Lability of enriched pFe

Scavenging of dFe onto particles has been considered a loss from the dissolved 'available' Fe pool, the consequences of which would be evident in the particulate fraction. Distinct enrichment of pFe over pAl, as indicated by raised pFe/pAl ratios (0.26-0.58; Fig.

176 1e), was observed in sub-surface waters (~25-50 m) at all stations except for the two coastal
177 stations (4 and 5). This pFe enrichment coincided with depths of maximum fluorescence (Fig.
178 S2), and is indicative of both biological Fe uptake as well as scavenging. Moreover,
179 enrichment of pFe (pFe/pAl >0.32) was observed down to 400 m and to a lesser degree
180 (pFe/pAl >0.30) down to 1000 m, encompassing the OMZ in a similar manner to dFe (Fig.
181 1e). The lability of the pFe fraction (Fig. S3) can provide an indication of the 'available'
182 particulate pool with a potential to impact dFe concentrations.. Our results demonstrate that
183 the Fe enrichment of particles was contained in the labile fraction, as indicated by the higher
184 Fe/Al ratios observed for labile particles compared to the refractory component. The average
185 refractory-pFe/pAl ratios in surface waters to the Chl *a* maximum, and down to 1100 m, were
186 close to the upper crustal ratio (0.21 ± 0.02; *n*=3 [*McLennan*, 2001; *Rudnick and Gao*, 2003;
187 *Wedepohl*, 1995]; Fig. 2a). In contrast, the average labile-pFe/pAl ratios at depths to the Chl
188 *a* maximum were elevated (0.30-1.73; Fig. 2a upper panel). At depths down to 1100 m this
189 Fe enrichment was even more distinct, with labile-pFe/pAl ratios ranging from 0.81 to 1.58
190 (Fig. 2a lower panel), indicating increased Fe scavenging onto particles with depth. Overall,
191 the leachable fraction (i.e. L-pFe/pFe x 100) ranged from 13–51% with a mean of 24% ± 6.5
192 (*n*=88) for all samples. A band of higher %L-pFe (~30%; Fig. 2b) was evident in the upper
193 water column (<400 m) where biological particle production and remineralization occurs.
194 Indeed positive correlations between L-pP and the biogenic elements of Cd (r^2=0.8278) and
195 Co (r^2=0.8947) were also observed here, a further indication of biological processes. Whilst
196 overall, pFe predominantly correlated with pAl (r^2=0.9867) and pTi (r^2=0.9780), in
197 agreement with previous studies [*Ohnemus and Lam*, 2015; *Twining et al.*, 2015], at depths
198 down to the Chl *a* maximum, L-pFe revealed a minor positive correlation with L-pP
199 (r^2=0.4176) indicating an association between L-pFe and biogenic matter in surface waters.

At depths >400 m, %L-pFe decreased to ~20% which may indicate a change in the nature of the pFe (Fig. 2b).

The distinct enrichment of L-pFe at the shelf stations (with labile-pFe/pAl ratios between 1.51 and 1.73; Fig. 2a) was dramatically higher than at any other station. Productivity in the shelf region was at least 2-fold higher than at any other station, with Chl *a* concentrations reaching up to 5.9 µg L^{-1}. Coastal phytoplankton have a higher requirement for Fe compared to oceanic species, and therefore store more Fe [*Brand*, 1991; *Maldonado and Price*, 1996; *Marchetti et al.*, 2006; *Sunda et al.*, 1991]. The high productivity in conjunction with local planktonic species has resulted in Fe-rich biogenic particles. Furthermore, direct input of dFe from bottom sediments would subsequently be scavenged in the particle abundant shelf region. Dissolved Fe had a similar distribution to the pFe phases in the shelf region, with elevated concentrations reaching 4-6 nM. Furthermore, raised dFe concentrations (1.2–6.3 nM) persisted throughout the water column and were evident as far west as station 6, a trend also observed for pFe. These enhanced dFe concentrations are not associated with any changes in the physical properties of the water column and most likely resulted from direct input of dFe from sediments and transport from the shelf [*Conway and John*, 2014], and/or dissolution from pFe.

3.3 Dynamic equilibrium between L-pFe and dFe

Comparison of pFe and L-pFe with dFe data in the OMZ revealed two distinct relationships as indicated by a 'kink' (Fig. 2c upper panels). Separating the stations into shelf influenced (stations 2–6, Fig. 2c middle panels) and open ocean (stations 7–9, 18, Fig. 2c bottom panels) indicates strong positive correlations between L-pFe and dFe throughout the transect (r^2=0.629 and 0.522, respectively). While a strong positive correlation was evident between pFe and dFe at the shelf influenced stations (r^2=0.6324), this was not similarly

maintained in open ocean waters (r^2=0.3605) whereby less than 40% of the variability in pFe could be explained by dFe. The change in slopes between shelf influenced and open ocean waters, reflects the differing oceanic environments; for example, a rise of 5.8 nM L-pFe nM^{-1} dFe would be expected at shelf influenced stations, in contrast to just 0.3 nM L-pFe nM^{-1} dFe in the open ocean, indicating a particle active regime closer to the shelf. This explains the strong relationship between both particle fractions and dFe in shelf influenced waters. Away from the shelf, while a strong relationship still exists, the changes in pFe concentrations are less correlated with those of dFe. However, regardless of region, concentrations of pFe dominate over those of dFe, thus enabling L-pFe to be an important conduit between pFe and the 'available' Fe pool. A recent model for the upper North Atlantic suggested that rates of sorption/desorption from particles were faster than biological uptake and remineralization rates [*John and Adkins,* 2012]. In our study region there is a large pool of pFe with supply from both shelf (Fig. 1b) and atmospheric sources. The relationships between L-pFe and dFe suggests that the two phases are intimately linked, most likely through dissolution and scavenging processes, resulting in an equilibrium i.e. where there is high L-pFe, exchange mechanisms with the dissolved phase can occur resulting in high dFe concentrations and vice versa. Indeed the distribution of dFe along this transect (Fig. 1d) in general reflects that of the particulate Fe phase.

The enhanced dFe concentrations in the OMZ have been attributed to remineralization of organic matter plus additional input of Fe from other particulate sources (e.g. atmospheric deposition) [*Fitzsimmons et al.,* 2013; *Rijkenberg et al.,* 2012; *Ussher et al.,* 2013]. A variable relationship between dFe and Apparent Oxygen Utilization (AOU) was observed for each station with r^2 values ranging from 0.3774 to 0.9963. This suggests that remineralization of Fe-containing biogenic particles, while variable, formed an important source of dFe. Calculation of Fe/C ratios by converting AOU to remineralised organic

carbon (applying an AOU/C ratio of 1.6 from Martin et al. [1989]) yielded Fe/C ratios in the range 9.2-41.6 μmol mol^{-1}. The lower values (9.2-11 μmol mol^{-1}) were representative of open ocean waters and are typical of Fe/C ratios reported for this region of the North Atlantic [*Fitzsimmons et al.*, 2013; *Rijkenberg et al.*, 2014; *Ussher et al.*, 2013]. These values are several fold higher than data from the low-Fe waters of the Pacific Ocean [*Sunda*, 1997], which has been attributed in part to luxury Fe uptake in North Atlantic waters [*Sunda*, 1997], however they are up to 4 fold lower than reported Fe/C ratios observed in phytoplankton in this region [*Twining et al.*, 2015] and bulk estimates of plankton Fe/C [*Kuss and Kremling*, 1999]. The discrepancy between our calculated Fe/C ratios (9.2-11 μmol mol^{-1}) and the higher observed values is attributed to scavenging and different rates of nutrient remineralization in the water column [*Hatta et al.*, 2015; *Twining et al.*, 2015]. We did however calculate higher Fe/C ratios for shelf influenced waters (16.1-41.6 μmol mol^{-1}) which are in a similar range to those reported by Twining et al. [2015]. These enhanced shelf influenced Fe/C values reflect additional dFe inputs, either from the shelf sediments and/or dissolution of pFe, or result from faster rates of pFe remineralization relative to C in the more productive shelf waters.

While remineralization is an important source of dFe in this region, the dFe-AOU regression analyses suggests that up to ~60% of the variance in dFe concentrations can be attributed to other sources or processes. Based on the relationship between L-pFe and dFe observed in our dataset, alongside the 20-30% L-pFe available for dissolution, we hypothesize that while Fe-binding ligands may control the solubility of dFe in the ocean, it is pFe and more specifically the labile fraction (L-pFe) which 'buffers' and ultimately controls dFe concentrations. If we therefore consider the L-pFe observed in the OMZ as part of the 'available' Fe pool, then at the outer most stations (7-9, 18) where the influence of the shelf

has diminished, this particulate fraction could increase the total available Fe (dFe + L-pFe) by up to 55%.

3.4 The significance of shelf derived Fe

The continental shelf in the OMZ of the (sub)-tropical North Atlantic is a distinct source for both particulate and dissolved Fe in this region (Fig. 1b,d). To further assess the significance of this shelf derived Fe supply, in comparison with dust deposition in the study area, fluxes for each were determined. Traditionally, only dFe has been accounted for in water column calculations, but as L-pFe can be considered as part of the 'available' Fe pool we have also calculated fluxes for this particulate fraction (see Methods). The differing magnitudes of these fluxes, split the transect into three zones; Shelf (Stations 4-5), Shelf-Influenced (Stations 3, 2, 6) and Open Ocean (Stations 7-9,18). The dFe and L-pFe fluxes for each of these zones were averaged and are shown along with our average soluble aerosol Fe flux (see Methods), obtained from samples collected during this study from the respective zone (Fig. 3). Full details of the estimated dFe and L-pFe fluxes for each station, are presented in the supplementary information (Table S2).

The total horizontal flux of Fe was highest in the Shelf zone where mean exports of dFe and L-pFe were estimated to be ~5,000 and 96,000 μmol m^{-2} d^{-1}, respectively. With increasing distance from the coast, the horizontal transport of dFe and L-pFe rapidly decreased, resulting in Open Ocean zone fluxes of 0.209 and 0.171 μmol m^{-2} d^{-1}, respectively. The near-shore lateral transport of dFe is one of the highest reported and is driven by the steep horizontal concentration gradient of dFe observed from the shelf to open ocean waters. Overall, our range of horizontal dFe fluxes for all stations (0.075–6700 μmol m^{-2} d^{-1}) are more variable than the range reported for a transect to the north of our study (33–288 μmol m^{-2} d^{-1} [*Rijkenberg et al.*, 2012]). The higher values were closer in magnitude to

those reported by de Jong et al. [2012] for a Southern Ocean region close to a continental shelf (~1400 μmol m^{-2} d^{-1}). Limited data are available for fluxes of particulate material, but our estimates are in agreement with those of Ratmeyer et al. [1999]. These workers reported horizontal advection for lithogenic material of 0.1 x 10^6 t y^{-1} off Cape Verde, adjusting this to include all particulate material (an increase of between 30–60% [*Ohnemus and Lam*, 2015]) and assuming that 25% relates to L-pFe then the flux estimates for our shelf stations were of a similar magnitude. While the horizontal transport of Fe decreased away from the Shelf, when combined as one 'available' Fe fraction, the flux of dFe and L-pFe (0.380 μmol m^{-2} d^{-1}) in the Open Ocean zone is greater than our soluble aerosol Fe deposition (0.135 ± 0.085 μmol m^{-2} d^{-1}, n=8). While these fluxes exert influence on different parts of the water column, this comparison reinforces the view that horizontal transport is important in this region and reiterates the emerging view that continental margins are an important supplier of nutrients and trace elements to ocean interiors [*Charette et al.*, 2016; *Lam et al.*, 2006].

For the horizontal Fe flux to impact ocean productivity and/or diazotrophy, vertical transfer into the surface mixed layer must occur. The calculated average vertical supply of dFe was greatest in the Shelf zone at 16 μmol m^{-2} d^{-1} and decreased to 0.022 μmol m^{-2} d^{-1} for the Open Ocean zone. Similarly, the calculated vertical flux of L-pFe decreased over the transect but was more dramatic, decreasing from 222 to 0.006 μmol m^{-2} d^{-1} from Shelf to the Open Ocean zones, respectively. The high vertical mixing in the shelf regions occurred where Fe concentration gradients were steepest, a result of dissolution, turbulence and sediment remobilization processes enriching overlying bottom waters in both Fe phases (e.g. ~6 nM of dFe and ~31 nM L-pFe). In general the overall concentrations of Fe in the water column were highest in this region, thus providing an enhanced Fe pool for transfer to surface waters. The calculated vertical supply of Fe into the surface mixed layer diminished over the transect and in the Open Ocean zone the dominant supply of Fe to surface waters, with an

estimated soluble flux of 0.135 μmol m^{-2} d^{-1} (Fig. 3), was aerosol deposition and agrees with the findings of recent studies [*Dammshauser et al.*, 2013; *Ohnemus and Lam*, 2015]. In general, our atmospheric flux estimates are very similar to the 10-year average flux of soluble Fe (0.117 μmol m^{-2} d^{-1}), calculated for our study region during the same sampling period, December to February [*Powell et al.*, 2015]. This seasonal average includes a substantial portion from wet deposition, a component which was not encountered during our own east-west transect, but is known to be an important constituent of atmospheric deposition in the (sub)-tropical North Atlantic [*Baker et al.*, 2007; *Buck et al.*, 2010; *Schlosser et al.*, 2014]. All atmospheric deposition is known to be highly transient and variable in intensity and our own dry deposition data show this, where in the two week period of sampling between occupation of stations 9 and 18, soluble Fe deposition decreased from 0.145 to 0.011 μmol m^{-2} d^{-1}, respectively. Compiling data from three previous studies that have reported soluble Fe from North African aerosols, and applying the same minimum and maximum deposition velocity used in our own flux calculations, results in an aerosol Fe flux estimate ranging from 0.001 μmol m^{-2} d^{-1} to 4.11 μmol m^{-2} d^{-1} [*Baker et al.*, 2013; *Buck et al.*, 2010; *Trapp et al.*, 2010]. As with any calculations, all of these flux estimates have uncertainties associated with them, and for atmospheric fluxes dry deposition velocity is a major uncertainty. Uncertainties aside, the lower of these estimates would certainly increase the importance of any additional Fe source to this region. Additionally, the bioavailable Fe fraction from dust is quickly utilized and its impact on productivity may be short lived (lasting ~2 weeks in studies from the subarctic Pacific [*Bishop et al.*, 2002]). Furthermore, recent studies relating to cellular quotas suggest that Fe availability from dust may be limited, and/or have a short residence time [*Ohnemus and Lam*, 2015; *Twining et al.*, 2015], in surface waters of the North Atlantic. During periods of low dust loadings, such as those experienced outside of the

winter months [*Powell et al.*, 2015], the potential supply of dFe and L-pFe from below could therefore constitute an additional important source of Fe.

4. Conclusions

Our results show that L-pFe can contribute a significant increase (up to 55%) to the overall 'available' Fe pool. The strong relationship between L-pFe and dFe indicates an equilibrium between the two phases, through dissolution and re-adsorption, whereby L-pFe buffers and maintains the high dFe concentrations observed in the open ocean waters of the OMZ. Lateral flux estimates for L-pFe are of a similar magnitude to dFe and aerosol sources, this reinforces the importance of pFe measurements and in particular the labile fraction. Particles, and most importantly the labile fraction, are integral to cycling and maintaining Fe bioavailability in the oceans, and therefore warrant inclusion in both Fe budgets and biogeochemical models. Given the key role of Fe in controlling oceanic productivity, accurate representations of Fe sources are crucial to predict ocean sensitivity to perturbations in the Fe cycle.

Acknowledgements

This project was funded by the UK Natural Environment Research Council NE/G016267/1 (Plymouth), NE/G015732/1 (Southampton) and NE/G016585/1 (East Anglia). The authors declare no competing financial interests. All data that supports the findings of this study have been submitted to the British Oceanographic Data Centre. The authors would like to thank the captain and crew of *RRS* Discovery and two anonymous reviewers for their valuable comments that helped improve this manuscript.

References

Baker, A. R., C. Adams, T. G. Bell, T. D. Jickells, and L. Ganzeveld (2013), Estimation of atmospheric nutrient inputs to the Atlantic Ocean from 50 degrees N to 50 degrees S based on large-scale field sampling: Iron and other dust-associated elements, *Glob. Biogeochem. Cycle*, *27*(3), 755-767, doi:10.1002/gbc.20062.

Baker, A. R., K. Weston, S. D. Kelly, M. Voss, P. Streu, and J. N. Cape (2007), Dry and wet deposition of nutrients from the tropical Atlantic atmosphere: Links to primary productivity and nitrogen fixation, *Deep Sea Res. Part I: Oceanogr. Res. Pap.*, *54*(10), 1704-1720, doi:10.1016/j.dsr.2007.07.001.

Berger, C. J. M., S. M. Lippiatt, M. G. Lawrence, and K. W. Bruland (2008), Application of a chemical leach technique for estimating labile particulate aluminum, iron, and manganese in the Columbia River plume and coastal waters off Oregon and Washington, *J. Geophys. Res.-Oceans*, *113*, doi:C00b01 10.1029/2007jc004703.

Bergquist, B. A., J. Wu, and E. A. Boyle (2007), Variability in oceanic dissolved iron is dominated by the colloidal fraction, *Geochim. Cosmochim. Acta*, *71*(12), 2960-2974, doi:10.1016/j.gca.2007.03.013.

Bishop, J. K. B., R. E. Davis, and J. T. Sherman (2002), Robotic observations of dust storm enhancement of carbon biomass in the North Pacific, *Science*, *298*(5594), 817-821, doi:10.1126/science.1074961.

Boyd, P. W., and M. J. Ellwood (2010), The biogeochemical cycle of iron in the ocean, *Nat. Geosci.*, *3*(10), 675-682, doi:10.1038/ngeo964.

Boyd, P. W., et al. (2012), Microbial control of diatom bloom dynamics in the open ocean, *Geophys. Res. Lett.*, *39*, doi:10.1029/2012gl053448.

Brand, L. E. (1991), Minimum iron requirements of marine-phytoplankton and the implications for the biogeochemical control of new production, *Limnol. Oceanogr.*, *36*(8), 1756-1771.

Bruland, K. W., K. J. Orians, and J. P. Cowen (1994), Reactive trace metals in the stratified central North Pacific, *Geochim. Cosmochim. Acta*, *58*(15), 3171-3182.

Buck, C. S., W. M. Landing, J. A. Resing, and C. I. Measures (2010), The solubility and deposition of aerosol Fe and other trace elements in the North Atlantic Ocean: Observations from the A16N CLIVAR/CO2 repeat hydrography section, *Mar. Chem.*, *120*(1-4), 57-70, doi:10.1016/j.marchem.2008.08.003.

Charette, M. A., et al. (2016), Coastal ocean and shelf-sea biogeochemical cycling of trace elements and isotopes: lessons learned from GEOTRACES, *Philosophical Transactions of the Royal Society A: Mathematical, Physical and Engineering Sciences*, *374*(2081), doi:10.1098/rsta.2016.0076.

Conway, T. M., and S. G. John (2014), Quantification of dissolved iron sources to the North Atlantic Ocean, *Nature*, *511*(7508), 212-215, doi:10.1038/nature13482.

Dammshauser, A., T. Wagener, D. Garbe-Schonberg, and P. Croot (2013), Particulate and dissolved aluminum and titanium in the upper water column of the Atlantic Ocean, *Deep Sea Res. Part I: Oceanogr. Res. Pap.*, *73*, 127-139, doi:10.1016/j.dsr.2012.12.002.

de Jong, J. T. M., V. Schoemann, D. Lannuzel, P. Croot, H. de Baar, and J. L. Tison (2012), Natural iron fertilization of the Atlantic sector of the Southern Ocean by continental shelf sources of the Antarctic Peninsula, *J. Geophys. Res.-Biogeosci.*, *117*, 25, doi:10.1029/2011jg001679.

Duce, R. A., P. S. Liss, J. T. Merrill, E. L. Atlas, P. Buat-Menard, B. B. Hicks, J. M. Miller, J. M. Prospero, R. Arimoto, and et al. (1991), The atmospheric input of trace species to the world ocean, *Glob. Biogeochem. Cycle*, *5*(3), 193-260, doi:10.1029/91gb01778.

Elrod, V. A., W. M. Berelson, K. H. Coale, and K. S. Johnson (2004), The flux of iron from continental shelf sediments: A missing source for global budgets, *Geophys. Res. Lett.*, *31*(12), art. no.-L12307.

Fitzsimmons, J. N., R. F. Zhang, and E. A. Boyle (2013), Dissolved iron in the tropical North Atlantic Ocean, *Mar. Chem.*, *154*, 87-99, doi:10.1016/j.marchem.2013.05.009.

Formenti, P., W. Elbert, W. Maenhaut, J. Haywood, and M. O. Andreae (2003), Chemical composition of mineral dust aerosol during the Saharan Dust Experiment (SHADE) airborne campaign in the Cape Verde region, September 2000, *J. Geophys. Res.-Atmos.*, *108*(D18), doi:10.1029/2002jd002648.

Ganzeveld, L., J. Lelieveld, and G. J. Roelofs (1998), A dry deposition parameterization for sulfur oxides in a chemistry and general circulation model, *J. Geophys. Res.-Atmos.*, *103*(D5), 5679-5694, doi:10.1029/97jd03077.

Gledhill, M., and C. M. G. van den Berg (1994), Determination of complexation of iron(III) with natural organic complexing ligands in seawater using cathodic stripping voltammetry, *Mar. Chem.*, *47*(1), 41-54.

Glover, D. M., W. J. Jenkins, and S. C. Doney (2011), *Modeling Methods for Marine Science*, Cambridge University Press, Cambridge, U.K., doi:10.1017/CBO9780511975721.

Hatta, M., C. I. Measures, J. Wu, S. Roshan, J. N. Fitzsimmons, P. Sedwick, and P. Morton (2015), An overview of dissolved Fe and Mn distributions during the 2010–2011 U.S. GEOTRACES north Atlantic cruises: GEOTRACES GA03, *Deep Sea Res. Pt. II: Top. Stud. Oceanogr.*, *116*, 117-129, doi:10.1016/j.dsr2.2014.07.005.

Homoky, W. B., S. Severmann, J. McManus, W. M. Berelson, T. E. Riedel, P. J. Statham, and R. A. Mills (2012), Dissolved oxygen and suspended particles regulate the benthic flux of iron from continental margins, *Mar. Chem.*, *134*, 59-70, doi:10.1016/j.marchem.2012.03.003.

Hong, H. S., and D. R. Kester (1986), Redox state of iron in the offshore waters of Peru, *Limnol. Oceanogr.*, *31*(3), 512-524.

Hurst, M. P., A. M. Aguilar-Islas, and K. W. Bruland (2010), Iron in the southeastern Bering Sea: Elevated leachable particulate Fe in shelf bottom waters as an important source for surface waters, *Cont. Shelf Res.*, *30*(5), 467-480, doi:10.1016/j.csr.2010.01.001.

Jickells, T. D. (1999), The inputs of dust derived elements to the Sargasso Sea; a synthesis, *Mar. Chem.*, *68*(1-2), 5-14.

Jickells, T. D., et al. (2005), Global iron connections between desert dust, ocean biogeochemistry, and climate, *Science*, *308*(5718), 67-71.

John, S. G., and J. Adkins (2012), The vertical distribution of iron stable isotopes in the North Atlantic near Bermuda, *Glob. Biogeochem. Cycle*, *26*, doi:10.1029/2011gb004043.

Klunder, M. B., P. Laan, R. Middag, H. J. W. De Baar, and J. C. van Ooijen (2011), Dissolved iron in the Southern Ocean (Atlantic sector), *Deep Sea Res. Pt. II: Top. Stud. Oceanogr.*, *58*(25-26), 2678-2694, doi:10.1016/j.dsr2.2010.10.042.

Kuss, J., and K. Kremling (1999), Spatial variability of particle associated trace elements in near-surface waters of the North Atlantic (30 degrees N/60 degrees W to 60 degrees N/2 degrees W), derived by large-volume sampling, *Mar. Chem.*, *68*(1-2), 71-86, doi:10.1016/s0304-4203(99)00066-3.

Lam, P. J., and J. K. B. Bishop (2008), The continental margin is a key source of iron to the HNLC North Pacific Ocean, *Geophys. Res. Lett.*, *35*(7), doi:L07608 10.1029/2008gl033294.

Lam, P. J., J. K. B. Bishop, C. C. Henning, M. A. Marcus, G. A. Waychunas, and I. Y. Fung (2006), Wintertime phytoplankton bloom in the subarctic Pacific supported by continental margin iron, *Glob. Biogeochem. Cycle*, *20*(1), doi:10.1029/2005gb002557.

Lam, P. J., D. C. Ohnemus, and M. E. Auro (2015), Size-fractionated major particle composition and concentrations from the US GEOTRACES north Atlantic zonal transect, *Deep Sea Res. Pt. II: Top. Stud. Oceanogr.*, *116*, 303-320, doi:http://dx.doi.org/10.1016/j.dsr2.2014.11.020.

Lippiatt, S. M., M. T. Brown, M. C. Lohan, C. J. M. Berger, and K. W. Bruland (2010), Leachable particulate iron in the Columbia River, estuary, and near-field plume, *Estuar. Coast. Shelf Sci.*, *87*(1), 33-42, doi:10.1016/j.ecss.2009.12.009.

Lippiatt, S. M., M. T. Brown, M. C. Lohan, and K. W. Bruland (2011), Reactive iron delivery to the Gulf of Alaska via a Kenai eddy, *Deep Sea Res. Part I: Oceanogr. Res. Pap.*, *58*(11), 1091-1102, doi:10.1016/j.dsr.2011.08.005.

Maldonado, M. T., and N. M. Price (1996), Influence of N substrate on Fe requirements of marine centric diatoms, *Mar. Ecol. Prog. Ser.*, *141*(1-3), 161-172.
Marchetti, A., M. T. Maldonado, E. S. Lane, and P. J. Harrison (2006), Iron requirements of the pennate diatom Pseudo-nitzschia: Comparison of oceanic (high-nitrate, low-chlorophyll waters) and coastal species, *Limnol. Oceanogr.*, *51*(5), 2092-2101.
Martin, J. H., R. M. Gordon, S. Fitzwater, and W. W. Broenkow (1989), Vertex - Phytoplankton / Iron Studies in the Gulf of Alaska, *Deep Sea Res. Part I: Oceanogr. Res. Pap.*, *36*(5), 649-680.
McLennan, S. M. (2001), Relationships between the trace element composition of sedimentary rocks and upper continental crust, *Geochem. Geophys. Geosyst.*, *2*, art. no.-2000GC000109.
Morel, F. M. M., A. J. Milligan, and M. A. Saito (2003), 6.05 - Marine Bioinorganic Chemistry: The Role of Trace Metals in the Oceanic Cycles of Major Nutrients., in *Treatise on Geochemistry*, edited by H. D. Holland and K. K. Turekian, pp. 113-143, Pergamon, Oxford, Unikted Kingdom.
Obata, H., H. Karatani, and E. Nakayama (1993), Automated determination of iron in seawater by chelating resin concentration and chemiluminescence detection, *Anal. Chem.*, *65*(11), 1524-1528.
Ohnemus, D. C., M. E. Auro, R. M. Sherrell, M. Lagerstrom, P. L. Morton, B. S. Twining, S. Rauschenberg, and P. J. Lam (2014), Laboratory intercomparison of marine particulate digestions including Piranha: a novel chemical method for dissolution of polyethersulfone filters, *Limnol. Oceanogr. Meth.*, *12*, 530-547, doi:10.4319/lom.2014.12.530.
Ohnemus, D. C., and P. J. Lam (2015), Cycling of lithogenic marine Particles in the US GEOTRACES north Atlantic transect, *Deep Sea Res. Pt. II: Top. Stud. Oceanogr.*, *116*, 283-302, doi:http://dx.doi.org/10.1016/j.dsr2.2014.11.019.
Powell, C. F., A. R. Baker, T. D. Jickells, H. W. Bange, R. J. Chance, and C. Yodle (2015), Estimation of the atmospheric flux of nutrients and trace metals to the eastern tropical North Atlantic Ocean, *J. Atmos. Sci.*, *72*(10), 4029-4045, doi:10.1175/jas-d-15-0011.1.
Ratmeyer, V., G. Fischer, and G. Wefer (1999), Lithogenic particle fluxes and grain size distributions in the deep ocean off northwest Africa: Implications for seasonal changes of aeolian dust input and downward transport, *Deep Sea Res. Part I: Oceanogr. Res. Pap.*, *46*(8), 1289-1337, doi:10.1016/s0967-0637(99)00008-4.
Revels, B. N., D. C. Ohnemus, P. J. Lam, T. M. Conway, and S. G. John (2015), The isotope signature and distribution of particulate iron in the North Atlantic Ocean, *Deep Sea Res. Pt. II: Top. Stud. Oceanogr.*, *116*, 321-331, doi:http://dx.doi.org/10.1016/j.dsr2.2014.12.004.
Rijkenberg, M. J. A., R. Middag, P. Laan, L. J. A. Gerringa, H. M. van Aken, V. Schoemann, J. T. M. de Jong, and H. J. W. de Baar (2014), The distribution of dissolved Iron in the West Atlantic Ocean, *PLOS One*, *9*(6), 14, doi:10.1371/journal.pone.0101323.
Rijkenberg, M. J. A., S. Steigenberger, C. F. Powell, H. van Haren, M. D. Patey, A. R. Baker, and E. P. Achterberg (2012), Fluxes and distribution of dissolved iron in the eastern (sub-) tropical North Atlantic Ocean, *Glob. Biogeochem. Cycle*, *26*, 15, doi:10.1029/2011gb004264.
Rudnick, R. L., and S. Gao (2003), 3.01 - The composition of the Continental Crust, in *Treatise on Geochemistry*, edited by H. D. Holland and K. K. Turekian, pp. 1-64, Pergamon, Oxford, United Kingdom, doi:http://dx.doi.org/10.1016/B0-08-043751-6/03016-4.
Rue, E. L., and K. W. Bruland (1995), Complexation of Iron(Iii) by Natural Organic-Ligands in the Central North Pacific as Determined by a New Competitive Ligand Equilibration Adsorptive Cathodic Stripping Voltammetric Method, *Mar. Chem.*, *50*(1-4), 117-138.
Schlosser, C., J. K. Klar, B. D. Wake, J. T. Snow, D. J. Honey, E. M. S. Woodward, M. C. Lohan, E. P. Achterberg, and C. M. Moore (2014), Seasonal ITCZ migration dynamically controls the location of the (sub)tropical Atlantic biogeochemical divide, *Proc. Natl. Acad. Sci. U.S.A.*, *111*(4), 1438-1442, doi:10.1073/pnas.1318670111.
Shelley, R. U., P. L. Morton, and W. M. Landing (2015), Elemental ratios and enrichment factors in aerosols from the US-GEOTRACES North Atlantic transects, *Deep Sea Res. Pt. II: Top. Stud. Oceanogr.*, *116*, 262-272, doi:http://dx.doi.org/10.1016/j.dsr2.2014.12.005.

522 Sunda, W. G. (1997), Control of dissolved iron concentrations in the world ocean: A comment, *Mar.*
523 *Chem.*, *57*(3-4), 169-172.
524 Sunda, W. G. (2001), Bioavailability and bioaccumulation of iron in the sea, in *The Biogeochemistry of*
525 *Iron in Seawater*, edited by D. R. Turner and K. A. Hunter, pp. 41-84, John Wiley & Sons Ltd,
526 Chichester.
527 Sunda, W. G., D. G. Swift, and S. A. Huntsman (1991), Low iron requirement for growth in oceanic
528 phytoplankton, *Nature*, *351*(6321), 55-57, doi:10.1038/351055a0.
529 Tagliabue, A., J. B. Sallee, A. R. Bowie, M. Levy, S. Swart, and P. W. Boyd (2014), Surface-water iron
530 supplies in the Southern Ocean sustained by deep winter mixing, *Nat. Geosci.*, *7*(4), 314-320,
531 doi:10.1038/ngeo2101.
532 Trapp, J. M., F. J. Millero, and J. M. Prospero (2010), Trends in the solubility of iron in dust-
533 dominated aerosols in the equatorial Atlantic trade winds: Importance of iron speciation and
534 sources, *Geochem. Geophys. Geosyst.*, *11*, 22, doi:10.1029/2009gc002651.
535 Twining, B. S., S. Rauschenberg, P. L. Morton, and S. Vogt (2015), Metal contents of phytoplankton
536 and labile particulate material in the North Atlantic Ocean, *Prog. Oceanogr.*, *137*, 261-283,
537 doi:10.1016/j.pocean.2015.07.001.
538 Ussher, S. J., E. P. Achterberg, C. Powell, A. R. Baker, T. D. Jickells, R. Torres, and P. J. Worsfold
539 (2013), Impact of atmospheric deposition on the contrasting iron biogeochemistry of the North and
540 South Atlantic Ocean, *Glob. Biogeochem. Cycle*, *27*(4), 1096-1107, doi:10.1002/gbc.20056.
541 Wedepohl, K. H. (1995), The composition of the continental crust, *Geochim. Cosmochim. Acta*, *59*(7),
542 1217-1232, doi:http://dx.doi.org/10.1016/0016-7037(95)00038-2.
543 Wells, M. L., N. M. Price, and K. W. Bruland (1995), Iron Chemistry in Seawater and Its Relationship
544 to Phytoplankton - a Workshop Report, *Mar. Chem.*, *48*(2), 157-182.
545 Whitfield, M. (2001), Interactions between phytoplankton and trace metals in the ocean, in
546 *Advances in Marine Biology, Vol 41*, edited by A. J. Southward, P. A. Tyler, C. M. Young and L. A.
547 Fuiman, pp. 1-128, Academic Press, doi:10.1016/s0065-2881(01)41002-9.
548 Wu, J. F., and G. W. Luther (1994), Size-fractionated iron concentrations in the water column of the
549 western North-Atlantic Ocean, *Limnol. Oceanogr.*, *39*(5), 1119-1129.

550

551

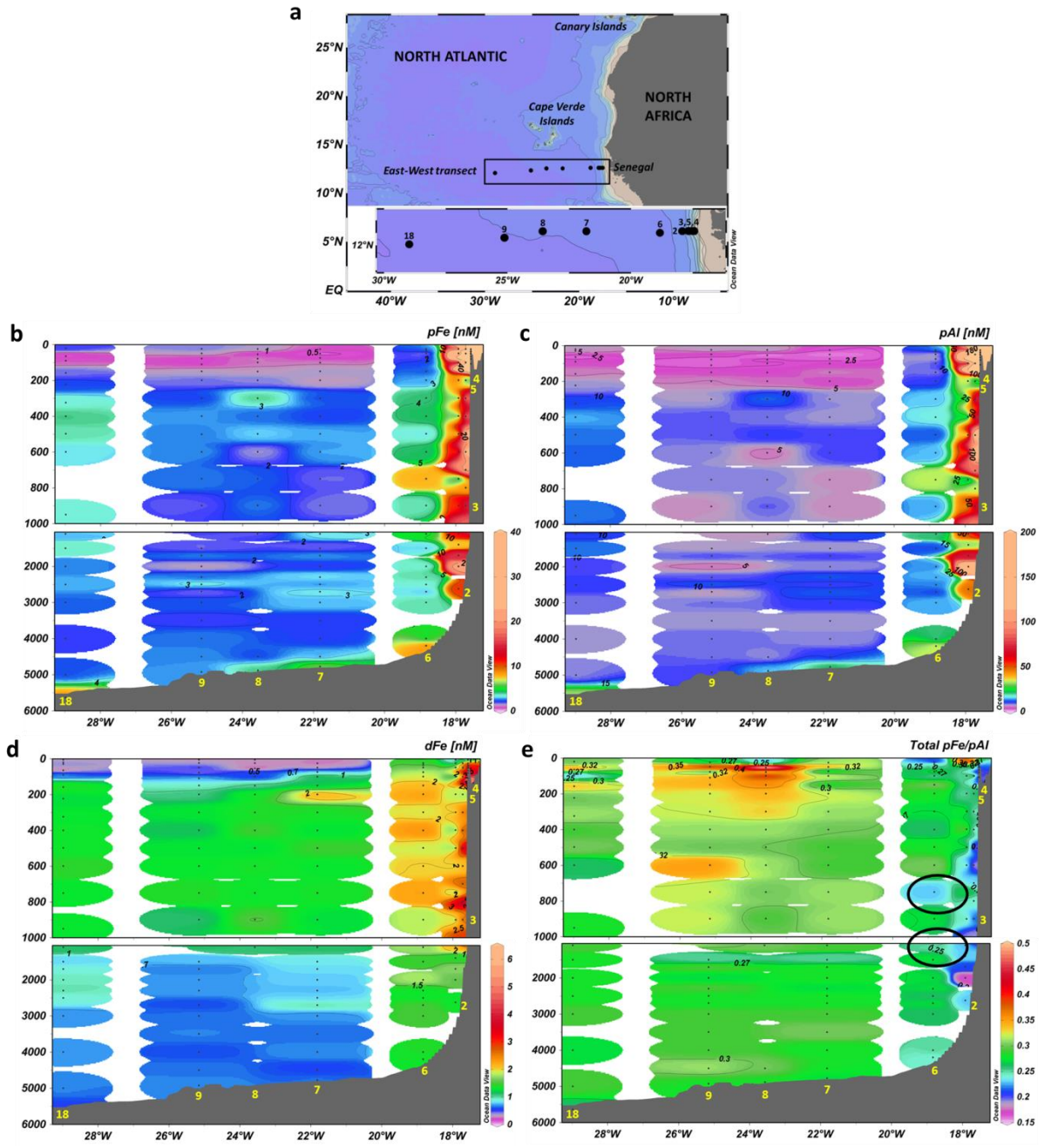

552

553 **Figure 1**. Location and profiles from the GEOTRACES A06 Cruise. (a) The transect along
554 12 ^{o}N is shown along with the sampling stations, (b) pFe, (c) pAl, (d) dFe, (e) the ratio of
555 pFe/pAl with the INLs at station 6 circled. Stations are numbered in yellow. Plots produced
556 using Ocean Data View (http://odv.awi.de).

557

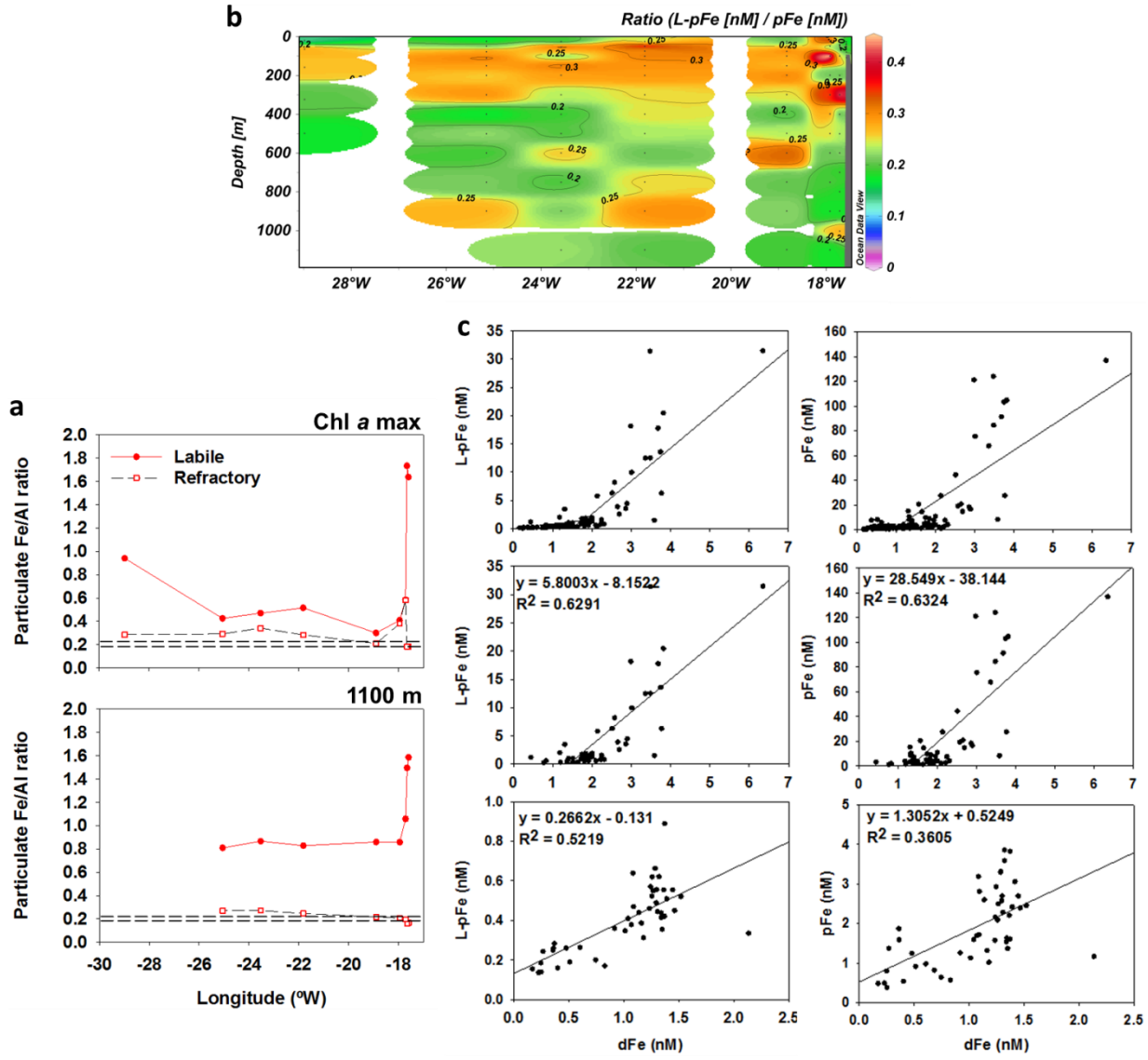

Figure 2. Labile-particulate Fe. (a) Enrichment of L-pFe (closed circles) over refractory pFe (open squares) is illustrated using Fe/Al ratios for the upper water column down to the Chl *a* maximum (upper panel) and from the bottom of the Chl *a* max to 1100 m (lower panel). The mol/mol crustal ratio range for Fe/Al of 0.19-0.23 is indicated by the dotted lines. (b) Distribution of labile particulate iron as a fraction of total p-Fe (L-pFe/pFe) in the upper 1100 m. (c) Relationship between dFe and L-pFe (left), and dFe and pFe (right) is shown for all stations (upper panels), shelf influenced stations 2–6 (middle panels) and open ocean stations 7–9, 18 (bottom panels). Note change in scales in the bottom panels.

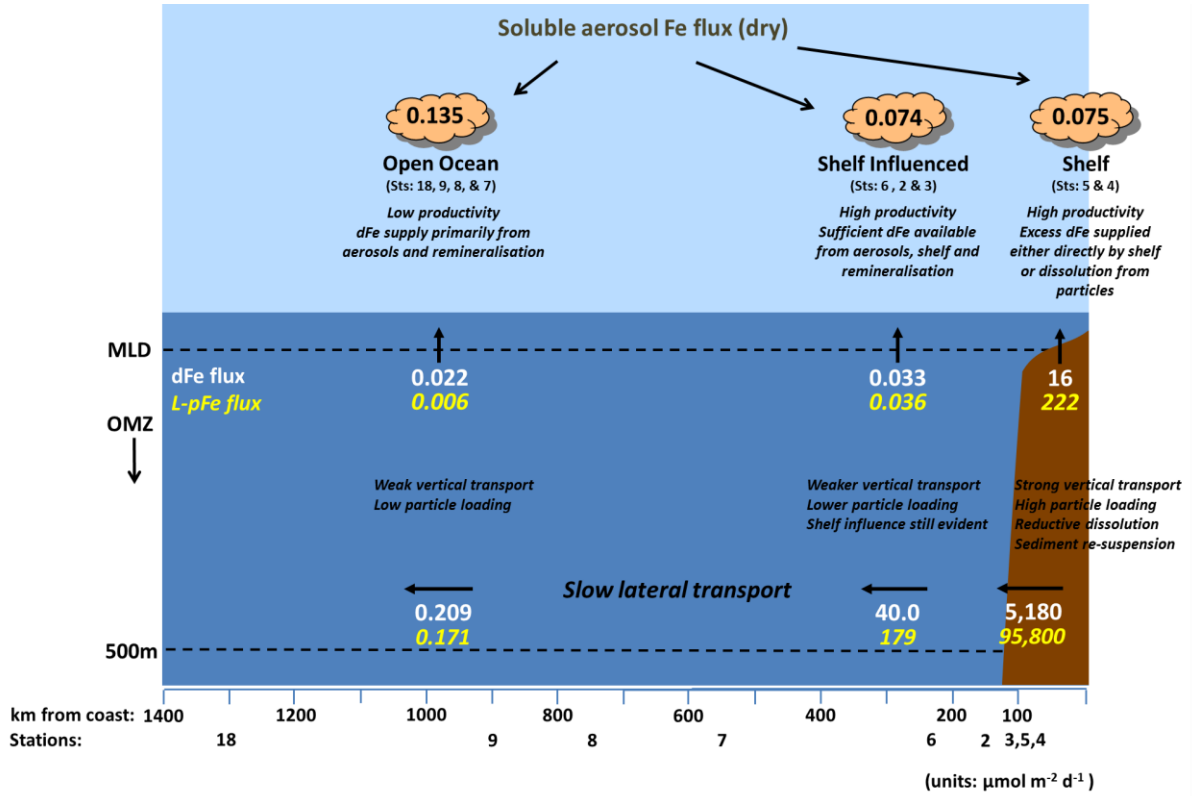

Figure 3. Schematic of fluxes of Fe. The nine stations were allocated into a zone (Shelf, Shelf Influenced and Open Ocean) and the averaged flux for that zone is shown. Fluxes for dFe are shown in white and L-pFe in yellow. All values are in µmol m^{-2} d^{-1}.